

A novel thymidine phosphorylase to synthesize (halogenated) anticancer and antiviral nucleoside drugs in continuous flow

Ana I. Benítez-Mateos,^a Calvin Klein,^a David Roura Padrosa,^a and Francesca Paradisi^{a*}

^a Department of Chemistry, Biochemistry and Pharmaceutical Sciences. University of Bern. Freiestrasse 3, 3012.
Bern (Switzerland)

Content:

Protein sequence of HeTP	3
Figure S1. SDS-PAGE analysis of the HeTP (48 kDa) expression at different conditions	3
Figure S2. Purification of HeTP by IMAC	4
Figure S3. Optimal conditions for the HeTP activity towards thymidine	5
Figure S4. Temperature stability of HeTP	6
Figure S5. Storage stability of HeTP	6
Figure S6. HeTP stability at different pH	7
Figure S7. A) Activity and B) stability of HeTP in presence of organic co-solvents	7
Figure S8. Phosphorolysis activity of HeTP towards thymidine	8
Figure S9. Michaelis Menten kinetics of HeTP towards thymidine and phosphate	8
Table S1. HeTP phosphorolysis activity with different purines	9
Table S2. HeTP phosphorolysis activity with different pyrimidines	10
Figure S10. Homology-modelled protein structure of HeTP	11
Figure S11. A) Docking of thymidine with WT HeTP and decitabine with the two mutants (R171E and R171Q). B) Evolution of the distance between the substrate and the binding residue	11
Site-directed mutagenesis of HeTP	12
Figure S12. Amino acid conservation analysis of the protein family <i>Glycos_transf_3</i> (PF00591)	12
Figure S13. SDS-PAGE analysis of the expression and purification of the variants A) HeTP-R171Q and B) HeTP-R171E	12
Figure S14. Biotransformations with 4'-amino substituted nucleosides	13
Figure S15. SDS-PAGE analysis of the covalently immobilized HeTP on premade supports	14
Figure S16. CapiPy analysis of HeTP	14
Figure S17. Reuses of the immobilized HeTP on different supports	15
Figure S18. Optimization of the HeTP loading on Gx-EP403/S	15
Figure S19. Temperature stability of the immobilized vs the free HeTP	16
Figure S20. DMSO stability of the immobilized HeTP on EP403/S	16
Figure S21. Optimization of A) the sugar donor concentration and B) phosphate concentration for the transglycosylation of 5-fluorouracil	17
Table S3. Testing the nucleobase concentration, the amount of biocatalyst, and the temperature to improve the transglycosylation yield	17
Table S4. Testing different nucleobase concentrations for the flow synthesis of Floxuridine	18
Table S5. Scale-up flow synthesis of Floxuridine	18
Figure S22. Operational stability of the immobilized HeTP on Gx-EP403/S (3 mg/g) under flow conditions	19
Supporting references	19

Protein sequence of HeTP expressed with 6x(His)tag

MGLPQEAIRAKRDGQALDAAAIGELVAGIADGSLGDAQIGALAMAIFLNGMNAETETVALTEAVRDSGD
VLDWTALDLPGPVIDKHSTGGVGDVVSLILGPWVAACGGHVP MISGRGLGHTGGTLDKLESIPGYSV
TPDTATFRRLVKDVGVAIIGQTADLAPADKRLYAIRDVTATVESLPLIVSSILGKKLACGLDALVMDVKV
GSGAFMPTPEASQELAETIAEVASRAGTPTTALLTMSQPLAPCAGNALEVHEALAVLTGKRPNRLL
EVTRGLAVEMLLAGGLAPDRDAALKRLDERLASGEEAERFGRMVAGLGGPADLLDAPDRHLPVAPV
VRPVLAPHAGHLRGLDTRALGMTVVELGGGRRQPGEAIDHAVGLADIAELGSKLDAGQPLATLHARS
HAEADQAERQLLEAIEIGEARPSPTLIRDIIIRREAPPNSSSVDKLA AALEHHHHHH

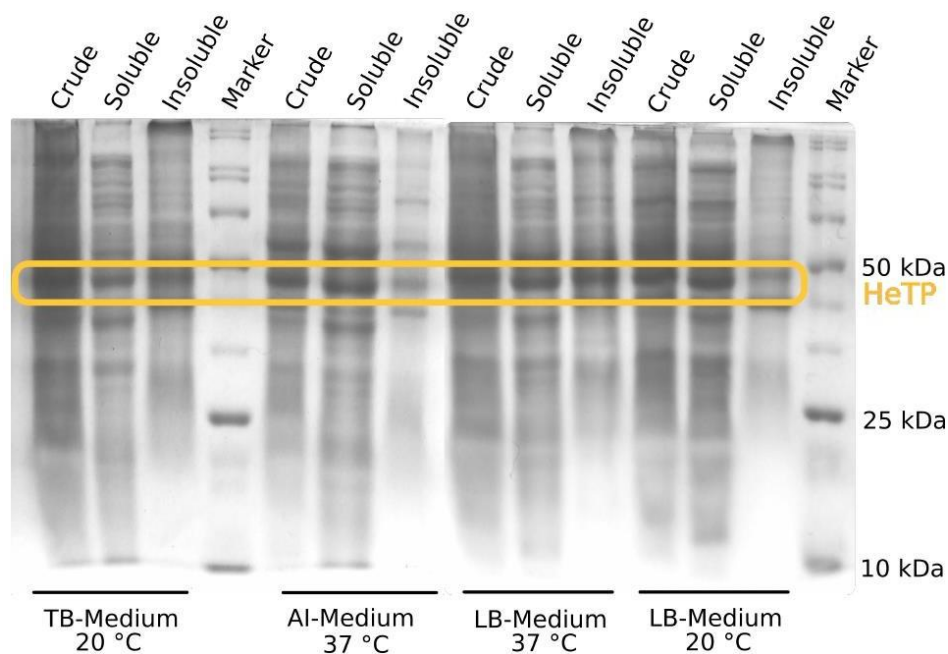
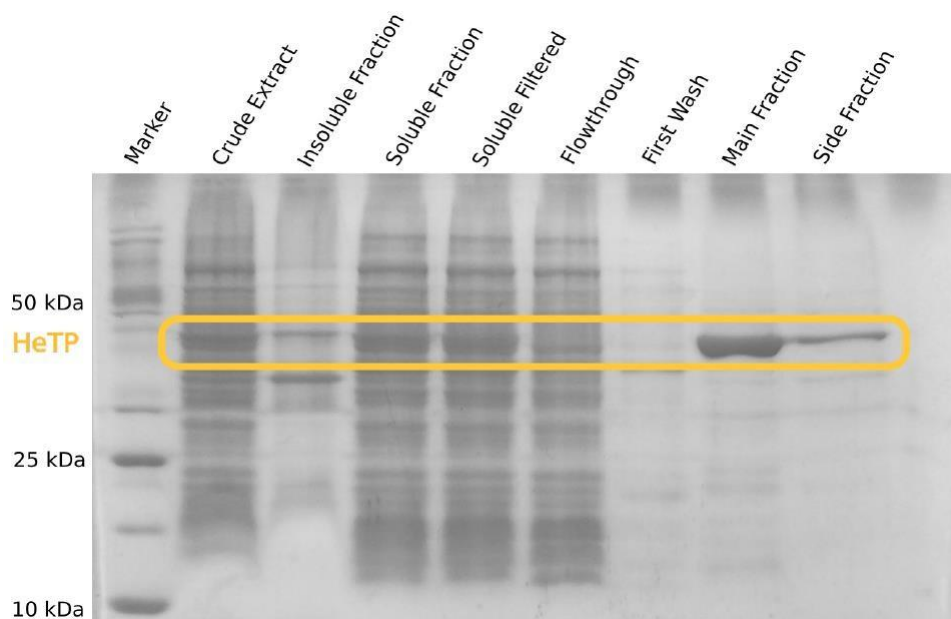


Figure S1. SDS-PAGE analysis of the HeTP (48 kDa) expression at different conditions. HeTP expression was tested in multiple media at different expression temperatures. The crude extract from *E. coli* BL21 (DE3) expressing HeTP, as well as the soluble and insoluble fractions of HeTP preparations after cell sonication were analysed by SDS-PAGE. HeTP bands are highlighted in gold at 48 kDa.

A**B**

Step	Total Protein (mg)	Total Enzyme Activity (U)	Specific Activity (U/mg)	Purification Fold	Yield
Crude Extract	72.9	305.8	4.2	1.0	100 %
Soluble Fraction	49.7	249.6	5.0	1.2	82%
IMAC	2.72	180.9	66.5	15.9	59 %

Figure S2. Purification of HeTP by IMAC. A) Various fractions produced during the purification steps were analysed by SDS-PAGE analysis. HeTP bands are highlighted in gold at 48 kDa. B) Purification results from a 2.3 g wet cell paste in autoinduction media. Protein concentrations were determined by the Bradford assay, and HeTP activities with 2.5 ng protein with 1 mM thymidine in 500 mM phosphate buffer. The purification fold was calculated using the specific activities of fractions produced during the purification steps, while the final yield was calculated from the total enzyme activity.

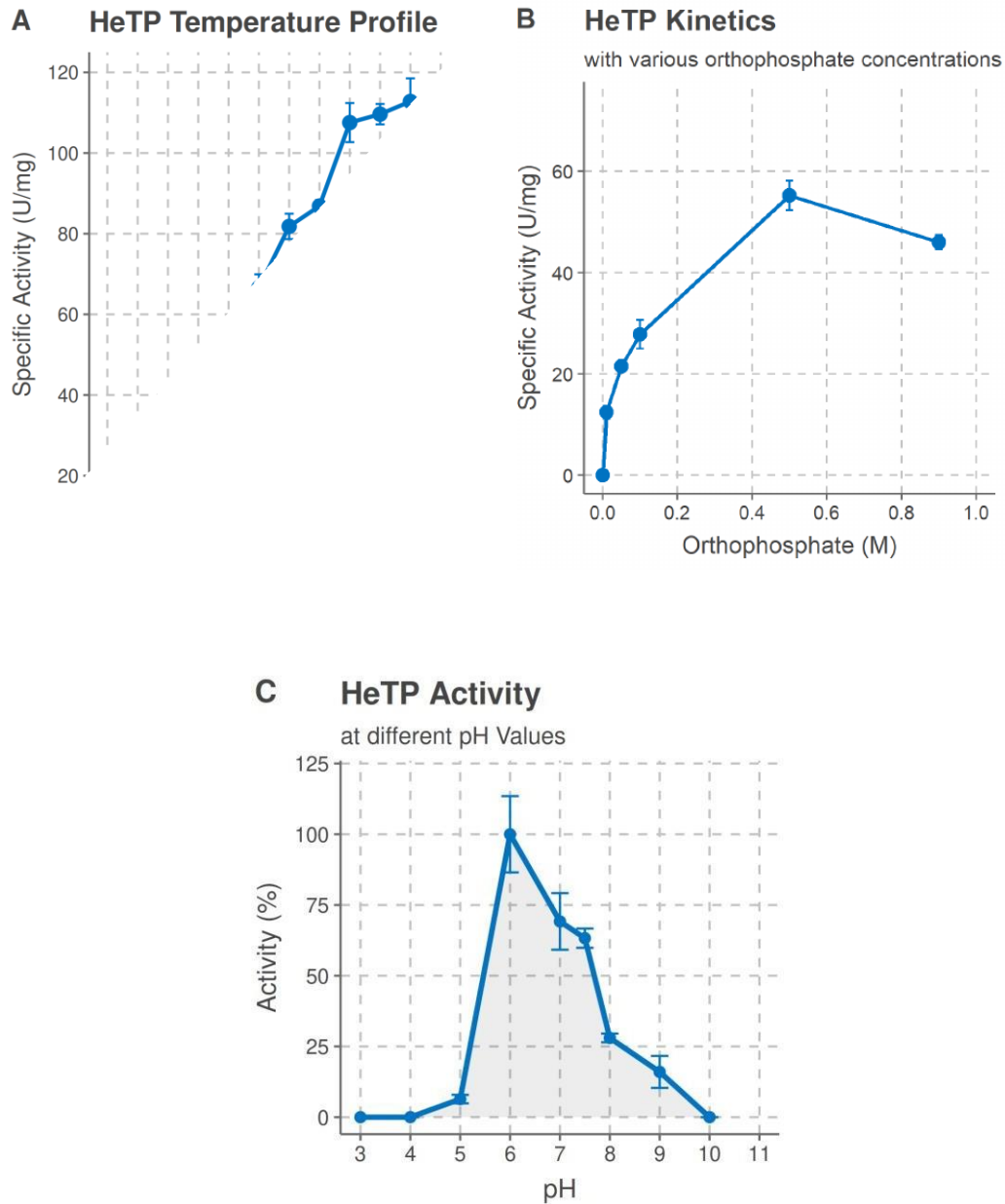


Figure S3. Optimal conditions for the HeTP activity towards thymidine. A) Activity of 2.5 ng HeTP with 1 mM thymidine in 500 mM phosphate, preheated to the indicated temperatures. B) Activity of 2.5 ng HeTP in the presence of 1 mM thymidine and varying phosphate concentrations in 50 mM HEPES buffer pH 7.5. C) Normalized activity of 2.5 ng HeTP with 1 mM thymidine in universal buffer (60 mM citric acid, 25 mM sodium tetraborate, 50 mM potassium chloride, 50 mM TRIS, 50 mM potassium phosphate) adjusted to various pH values. 100 % activity equals 14.5 U/mg. All measurements were done in 3 technical replicates. Error bars represent standard deviation.

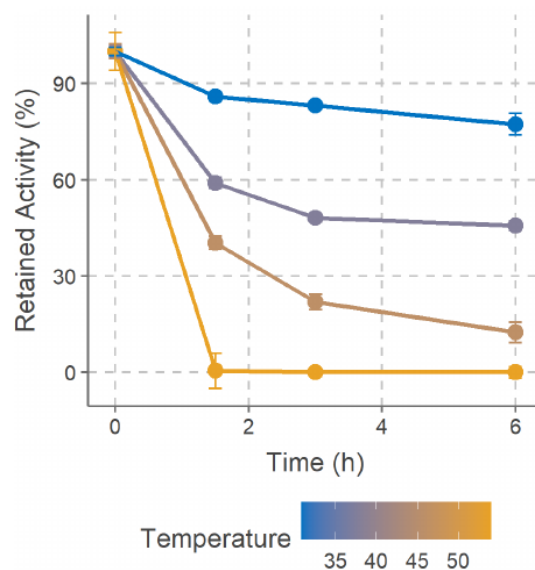


Figure S4. Temperature stability of HeTP. HeTP was incubated at different temperatures between 30 and 55 °C using a PCRmax Alpha. After the indicated times, reactions were performed with 2.5 ng HeTP and 1 mM thymidine in 500 mM phosphate buffer at pH 7.0. All measurements were done in 3 technical replicates. Error bars represent standard deviation.

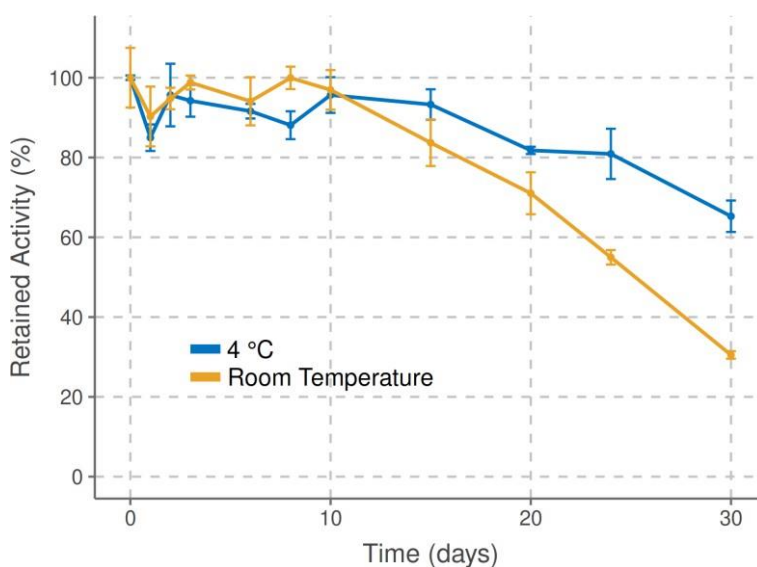


Figure S5. Storage stability of HeTP. HeTP aliquots were stored at the 4 °C and at room temperature. After the indicated timepoints activities were measured with 2.5 ng HeTP and 1 mM thymidine in 500 mM phosphate buffer. Measurements were performed in 3 technical replicates. Error bars represent standard deviation.

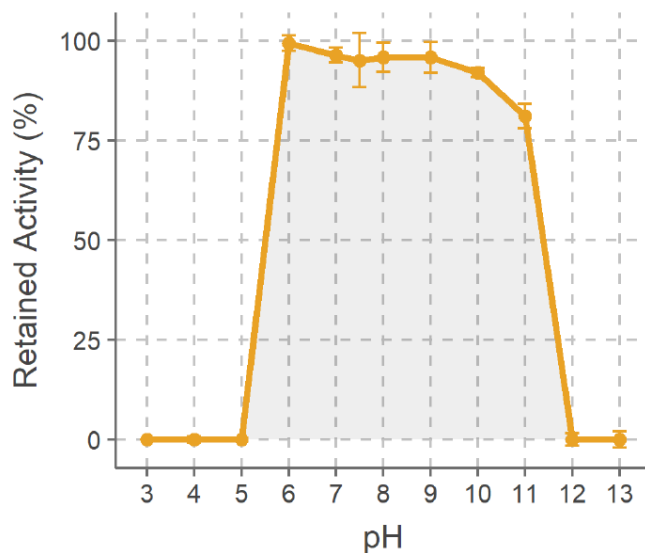
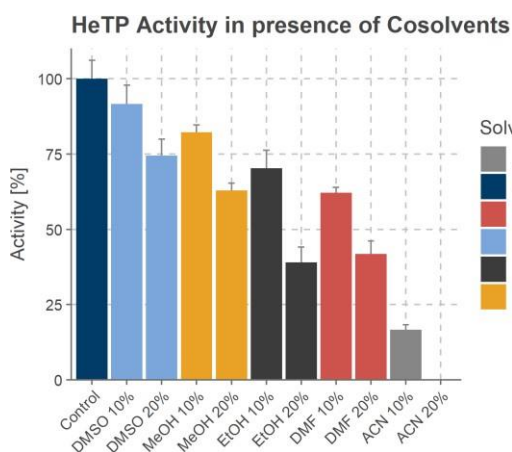


Figure S6. HeTP stability at different pH. HeTP was prepared in universal buffer (60 mM citric acid, 25 mM sodium tetraborate, 50 mM potassium chloride, 50 mM TRIS) adjusted to the shown pH values. After one hour of incubation, activities were measured with 2.5 ng HeTP and 1 mM thymidine in phosphate buffer. Measurements were performed in 3 technical replicates. Error bars represent standard deviation.

A



B

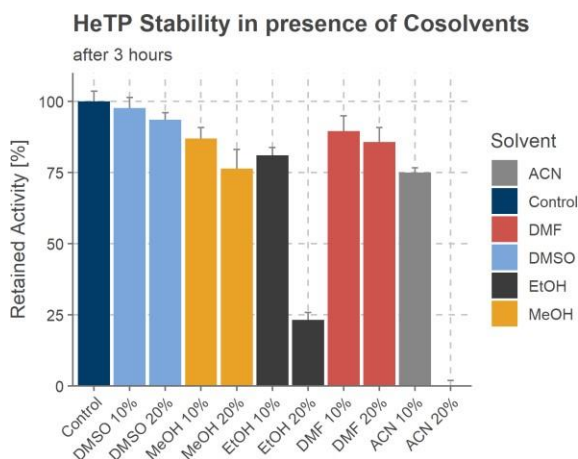


Figure S7. A) Activity and B) stability of HeTP in presence of organic co-solvents. A) HeTP activity was assessed with 2.5 ng HeTP with 1 mM thymidine in 50 mM phosphate buffer supplemented with the indicated amount organic solvent. 100 % activity equals 28.79 U/mg. B) Purified HeTP was diluted with buffer or 10-20 % indicated solvent. After 3 hours of incubation at room temperature, the retained activity was assessed with 2.5 ng HeTP and 1 mM thymidine in 500 mM phosphate buffer. 100 % activity equals 58.2 U/mg. All measurements were done in 3 technical replicates. Error bars represent standard deviation.

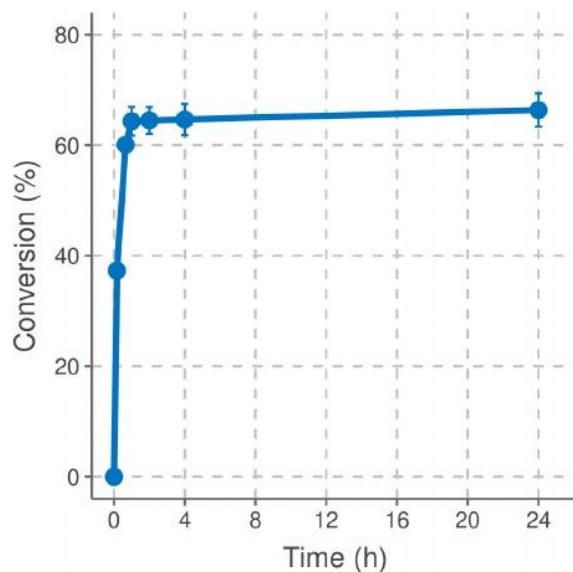


Figure S8. Phosphorolysis activity of HeTP towards thymidine. A) Phosphorolysis of 5 mM thymidine in 500 mM phosphate buffer, using 2.5 ng purified HeTP. Measurements were done in 3 technical replicates. Error bars represent standard deviation.

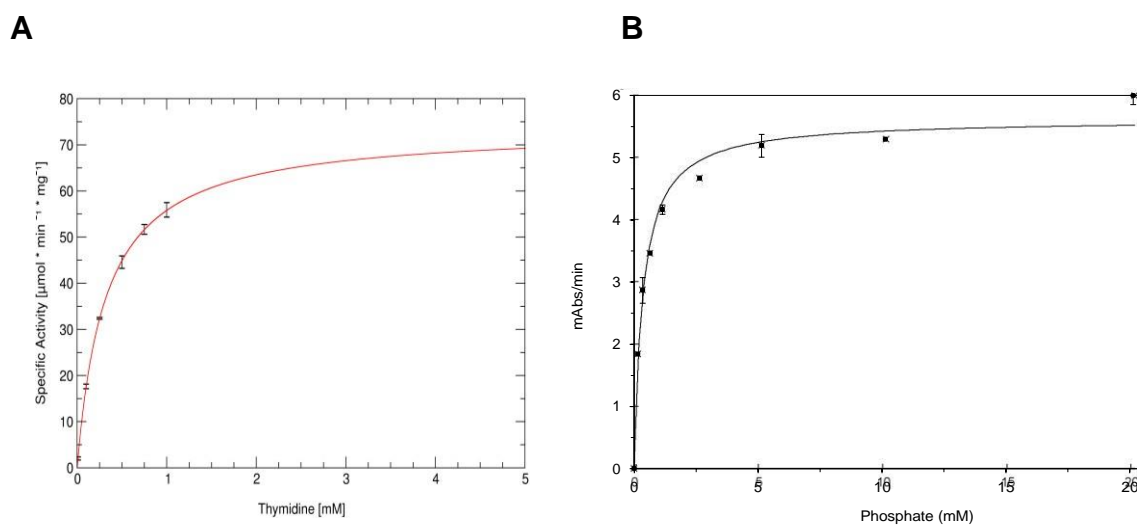


Figure S9. Michaelis Menten kinetics of HeTP towards thymidine and phosphate. A) 2.5 ng of purified HeTP were added to 1 mL of 500 mM phosphate buffer with varying thymidine concentrations. V_{Max} : 73 U/mg, K_M : 0.32 mM. Measurements were done in 3 technical replicates. Error bars represent standard deviation. Significance of the extrapolated activity: $p < 0.001$. B) 10 μL of HeTP (0.25 mg/mL) were mixed with 0.2-20 mM phosphate in 100 mM HEPES buffer at pH 7.0 containing 3 mM thymidine. Absorbance at 290 nm was monitored for 10 min. An estimated K_M : 0.36 mM was determined. V_{Max} could not be determined with this method as the absorbance values were over 3 AU. Error bars represent standard deviation.

Table S1. HeTP phosphorolysis activity with different purines. Activities were determined with 5 mM substrate in the presence of 50 mM phosphate, 5% DMSO, using 250 µg purified HeTP. Sample analysis was performed by HPLC. not detected (n.d.). Measurements were performed in duplicates.

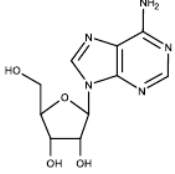
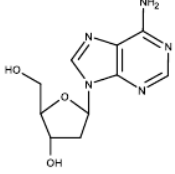
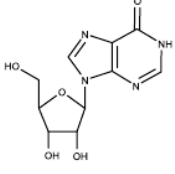
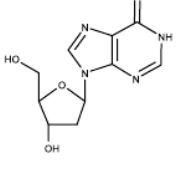
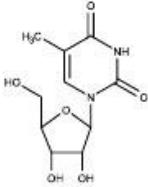
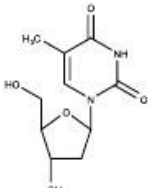
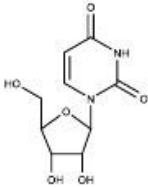
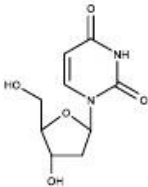
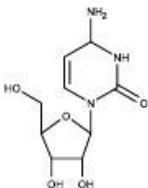
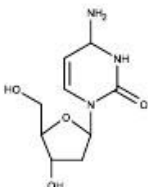
NUCLEOSIDE	SPECIFIC ACTIVITY (U/MG)	STRUCTURE
Adenosine	n.d.	
Deoxyadenosine	n.d.	
Inosine	n.d.	
Deoxyinosine	n.d.	

Table S2. HeTP phosphorolysis activity with pyrimidines. Activities were determined with 5 mM substrate in the presence of 50 mM phosphate, 5% DMSO, using 250 µg purified HeTP. Sample analysis was performed by HPLC. not detected (n.d.). Measurements were performed in duplicates.

NUCLEOSIDE	SPECIFIC ACTIVITY (U/MG)	STRUCTURE
5-Methyluridine	n.d.	
Thymidine	35.21 ± 2.59	
Uridine	n.d.	
Deoxyuridine	65.44 ± 2.59	
Cytidine	n.d.	
Deoxycytidine	n.d.	

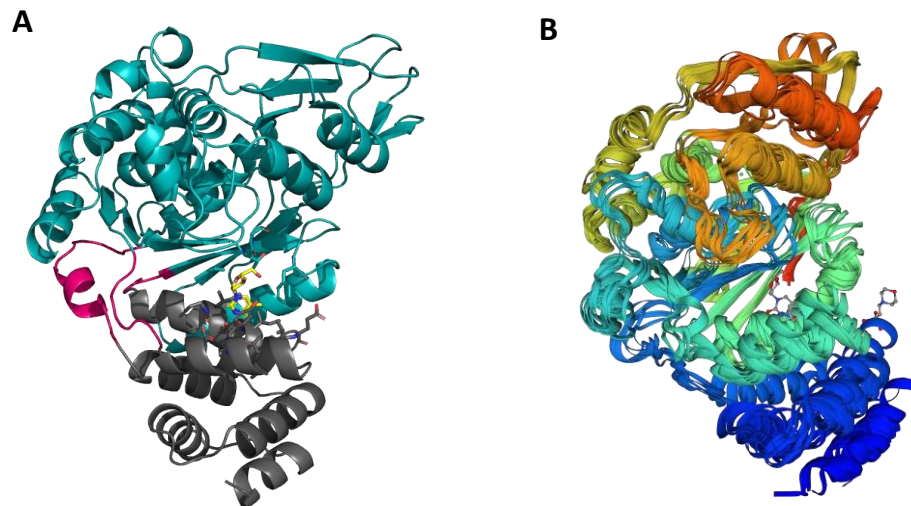


Figure S10. Homology-modelled protein structure of HeTP. A) Cartoon representation of the HeTP homology model based on PyNP from *S. aureus* (PDB: 3H5Q). The α - β -domain (cyan) is connected to the α -domain (dark gray) via a hinge region (magenta). In the active site, thymidine (yellow) is bound. B) Superposition of PyNPs and TPs originating from various organisms. 7 crystal structures with sequence identities between 30 % and 60 % to HeTP were superimposed: *E. coli* TP (PDB: 2TPT), *B. subtilis* PyNP (PDB: 5EP8), *S. thyphimurium* TP (PDB: 4XR5), *B. stearothermophilus* PyNP (PDB: 1BRW), *S. aureus* PyNP (PDB: 3H5Q), *T. thermophilus* PyNP (PDB: 2DSJ) and *H. sapiens* TP (PDB: 2WK6).

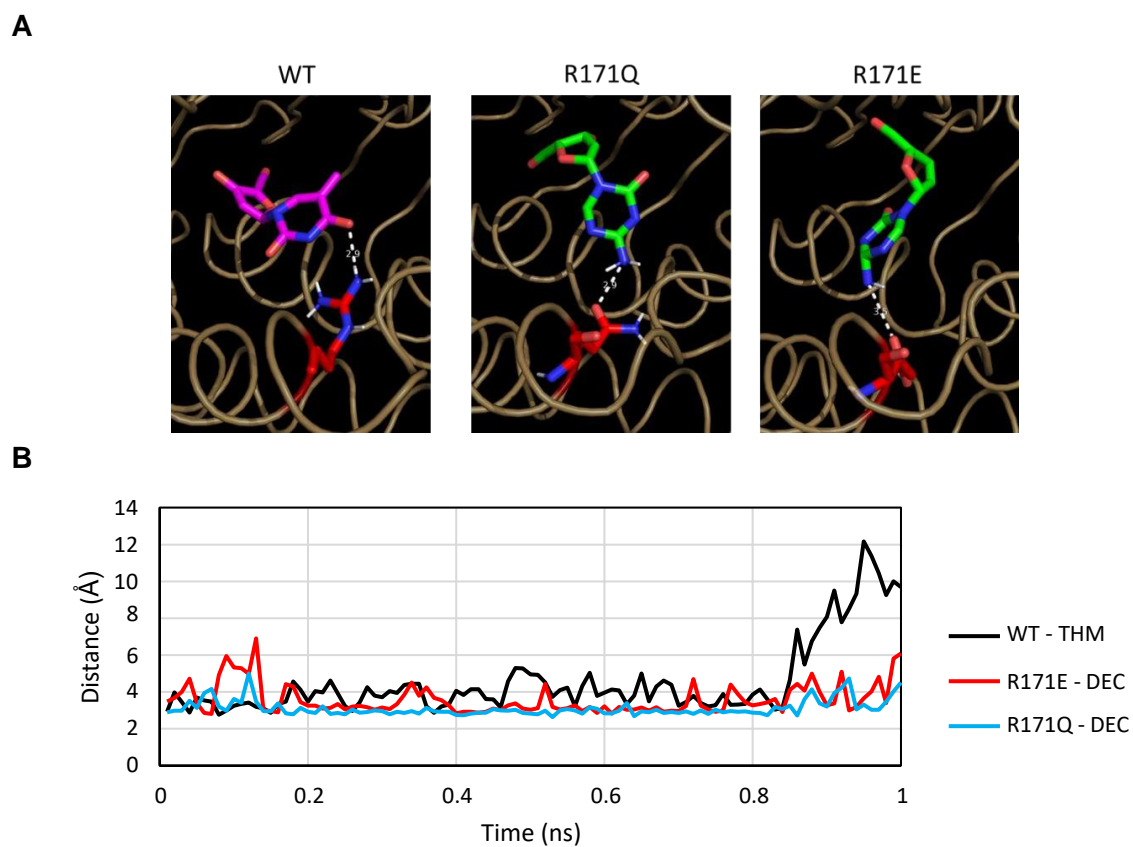


Figure S11. A) Docking of thymidine with WT HeTP and decitabine with the two mutants (R171E and R171Q). Thymidine is shown in dark pink and Decitabine in green. The key residue for the stabilization of either the oxygen for thymidine or the primary amine in Decitabine are coloured in red, and the distance is shown. **B) Evolution of the distance between the substrate and the binding residue.**

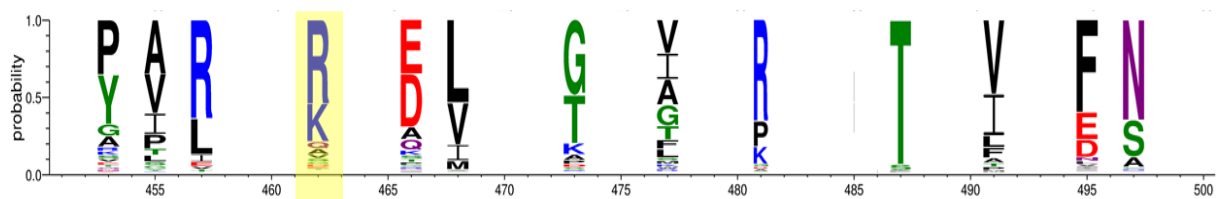


Figure S12. Amino acid conservation analysis of the protein family *Glycosyl transferase 3* (PF00591). The position R171 is highlighted in yellow. 14,382 protein sequences were aligned with Pfam. Conservation analysis was performed with Bioedit and weblogo3.

Site-directed mutagenesis of HeTP

The mutants HeTP R171E and HeTP R171Q were generated by using the Q5® Site-directed mutagenesis kit from NEB, following the manufacturer protocol. The following primers were used:

- R171E
 F: 5'-TGTATGCGATCGAAGACGTGACCGCGACCGTTGAAAG-3'
 R: 5'-GACGTTTATCCGCCGGCGCCAGGTC-3'
- R171Q
 F: 5'-TGTATGCGATCCAGGACGTGACCGCGAC-3'
 R: 5'-GACGTTTATCCGCCGGCGCCAGGTC-3'

All the mutations were verified by Sanger sequencing at Microsynth.

The mutated proteins were expressed in *E. coli* and purified by IMAC (Fig. S13).

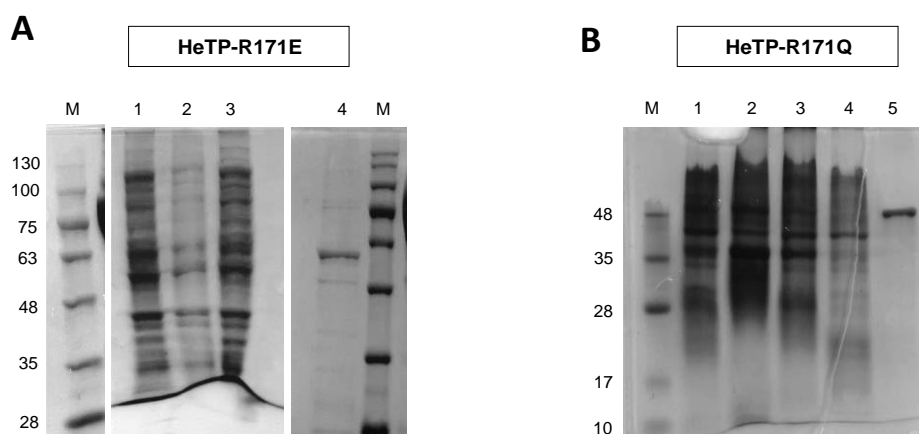


Figure S13. SDS-PAGE analysis of the expression and purification by IMAC of the variants A) HeTP-R171Q and B) HeTP-R171E. For A), 1: total protein, 2: insoluble fraction, 3: soluble fraction, 4: purified fraction; for B) 1: total protein, 2: insoluble fraction, 3: soluble fraction, 4: flow-through during the purification (unbound fraction), 5: purified fraction. M: protein ladder from BIORAD.

Among the 4-amino substituted nucleoside drugs, we targeted Decitabine as it is a 2'-deoxy nucleoside, thus it could potentially be synthesized by HeTP. We tested the phosphorolysis of the 5-amino nucleosides by using the two variants and the WT-HeTP as control. HeTP-R171E did not show activity towards any of the nucleoside analogues tested. We hypothesized that this issue could be solved using the variant HeTP-R171Q, as the dual functionality of the side chain of Gln could stabilize the transition state of the nucleobase and it could also hydrogen-bond the 4-amino position. In fact, HeTP-R171Q showed 10% of activity towards thymidine compared to the wild-type (WT) HeTP, although no activity towards 4-amino substituted substrates was detected (Fig. S14A). Then, we coupled the phosphorolysis of thymidine by the WT-HeTP to the transglycosylation of the 4-amino nucleobase by R171E-HeTP or R171Q-HeTP. Although the phosphorolysis worked as expected in all cases, the transglycosylation was unsuccessful (Fig. S14B). Most likely, the negative charge generated following phosphorolysis of the glycosidic bond still needs the positive charge of R171 to be stabilized.^{11,2}

Note that Decitabine could not be detected by HPLC. Then, we observed that Decitabine was unstable under aqueous solution in agreement with previous studies that described its degradation over time.^{3,4} However, a recent study has reported the biosynthesis of Decitabine in aqueous solution with similar reaction conditions to the present work.⁵

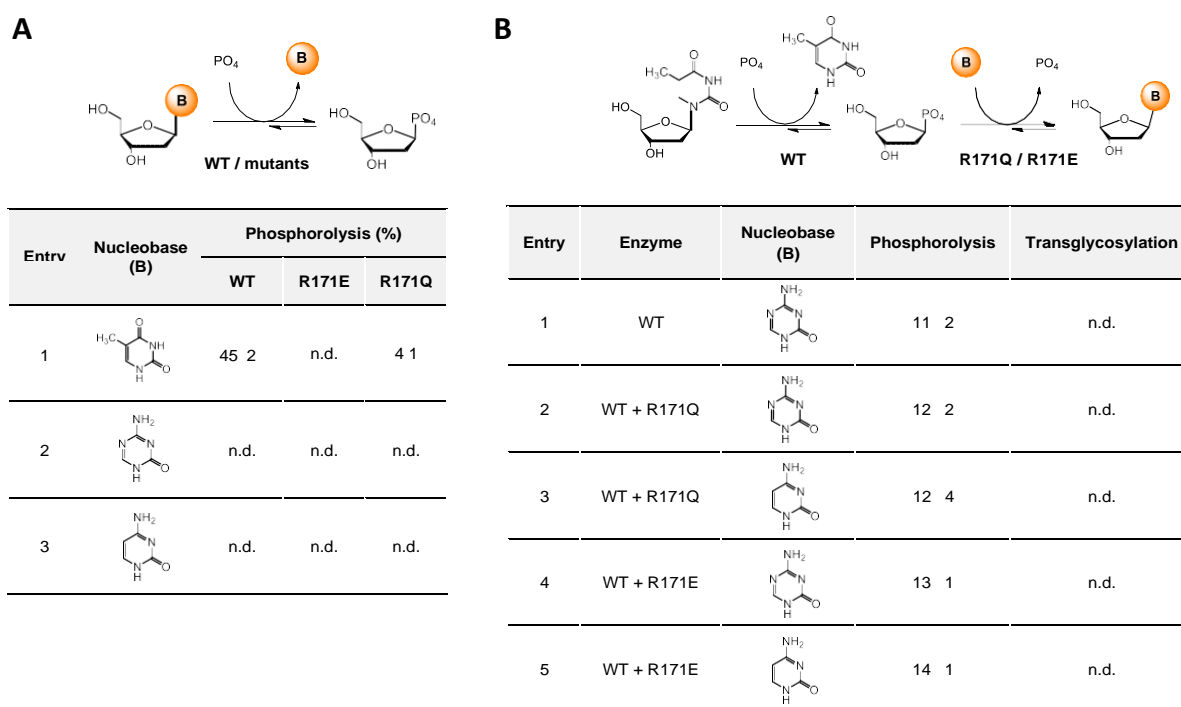


Figure S14. Biotransformations with 4'-amino substituted nucleosides. On the top, the reaction schemes. A) Phosphorolysis of thymidine (entry 1), Decitabine (entry 2), deoxycytidine (entry 3). 0.1 mg of HeTP were added in 0.5 mL containing 20 mM nucleoside in 500 mM phosphate buffer pH 7.0. B) Phosphorolysis of thymidine using the HeTP-WT and transglycosylation reaction by using either the variant HeTP-R171E or HeTP-R171Q. 0.2 mg of HeTP (WT and mutant) were added in 0.5 mL containing 5 mM nucleobase, 100 mM thymidine in 10 mM phosphate buffer pH 7.5. All the reactions were incubated at 37 °C for 24 h with shaking. n.d: not detected.

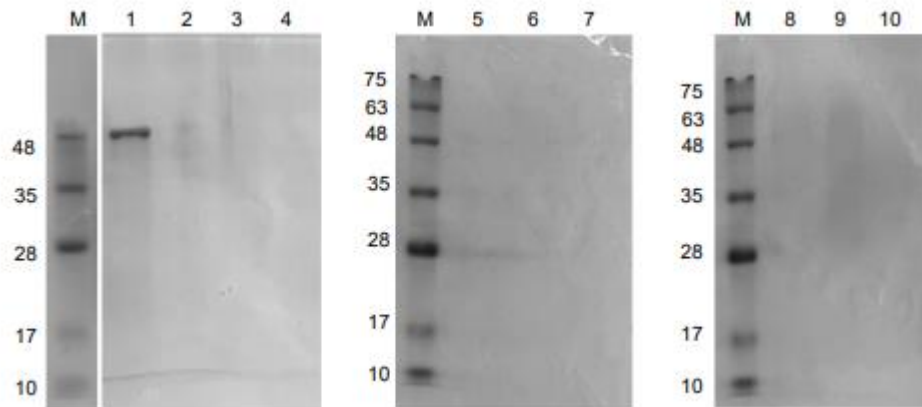


Figure S15. SDS-PAGE analysis of the covalently immobilized HeTP on pre-made supports. 1: offered HeTP for immobilization, 2: flow-through after immobilization on Gx-EP400/SS, 3: flow-through after immobilization on Gx-AG, 4: flow-through after immobilization on Gx-EP403/S, 5: flow-through after immobilization on Ep-EP403/S, 6: HeTP immobilized on Gx-EP403, 7: HeTP immobilized on Gx-EP400/SS, 8: HeTP immobilized on Ep-EP403/S, 9: HeTP immobilized on Gx-AG, 10: HeTP immobilized on Ep-AG, M: protein ladder from Geneaid.

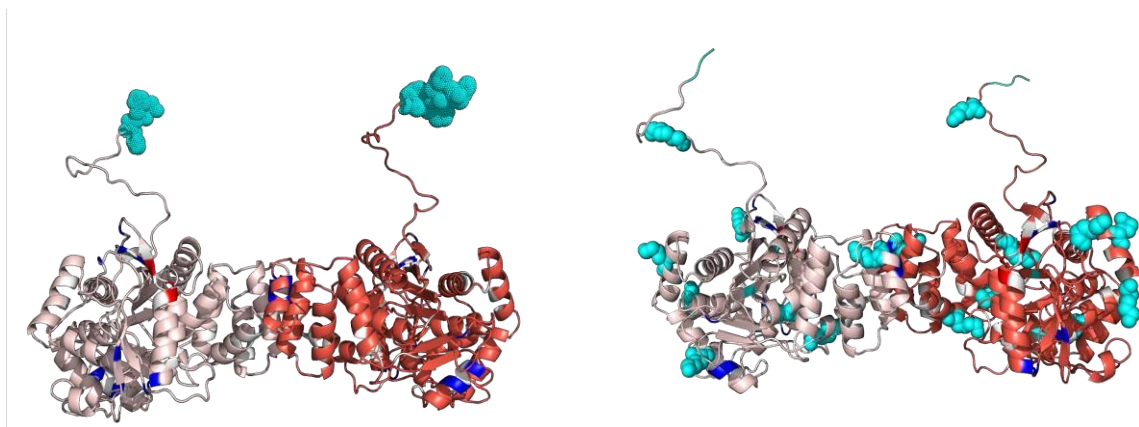


Figure S16. CapiPy⁶ analysis of HeTP. **A.** Representation of the location of the His-tag coloured in cyan and shown as dotted spheres in HeTP. **B.** Distribution of the lysine residues in the surface of HeTP, coloured in cyan and shown as spheres.

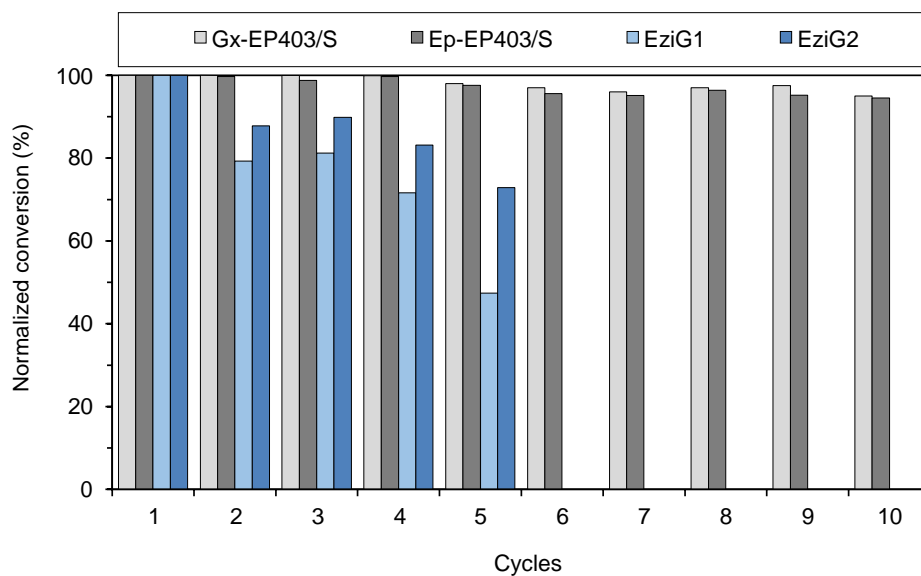


Figure S17. Reuses of the immobilized HeTP on different supports. 50 mg of immobilized HeTP (1 mg/g) were added in 1 mL of 5 mM thymidine in 500 mM phosphate buffer pH 7.5. The reaction was maintained at 37°C for 1 h.

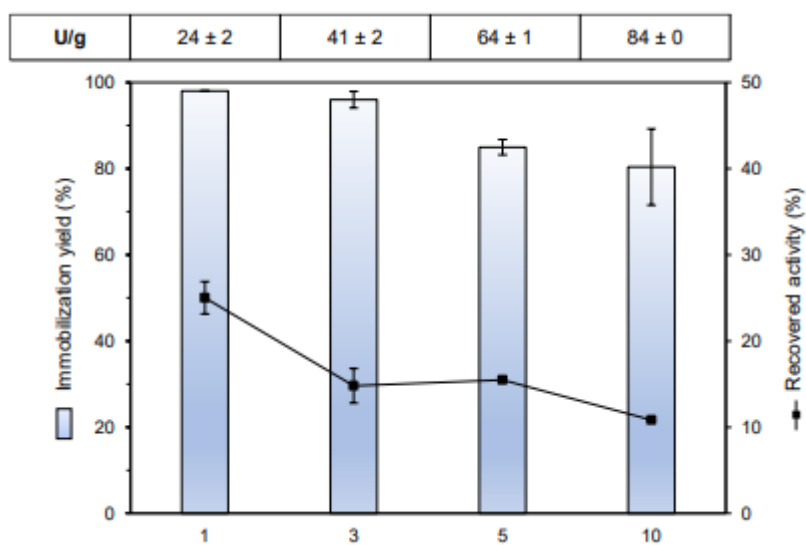


Figure S18. Optimization of the HeTP loading on Gx-EP403/S. The expressed activity is depicted as U/g. Error bars represent standard deviation.

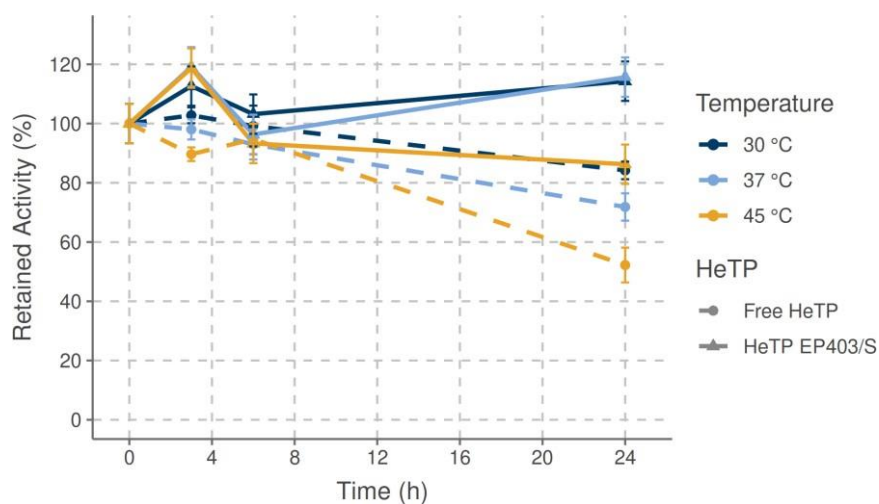


Figure S19. Temperature stability of the immobilized vs the free HeTP. For immobilized HeTP, 20 mg of immobilized HeTP (1 mg/g), incubated at the indicated temperature, were added to 2.5 mL of 1 mM thymidine in 500 mM phosphate buffer pH 7.0. For free HeTP, 10 μ L of HeTP (0.25 mg/mL), incubated at the indicated temperature, were added to 1 mL of 1 mM thymidine in 500 mM phosphate buffer pH 7. The reactions were followed at 290 nm and 30 °C for 1 min. Error bars represent standard deviation of technical triplicates.

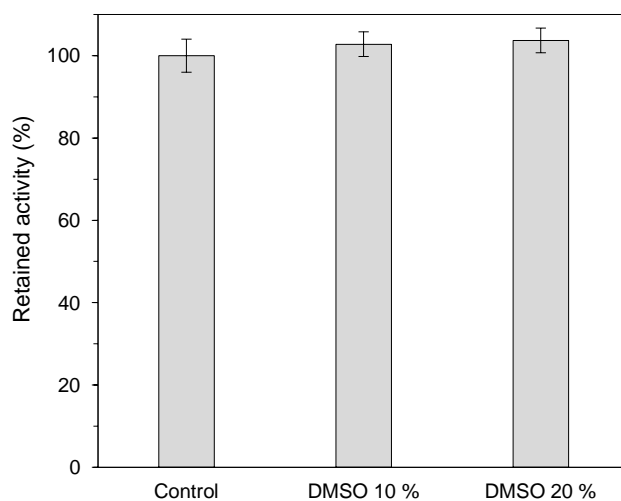


Figure S20. DMSO stability of the immobilized HeTP on EP403/S. The immobilized enzyme was incubated in 50 mM phosphate buffer pH 7.0 containing the indicated DMSO percentage. The control sample did not contain DMSO. Error bars represent standard deviation of technical triplicates.

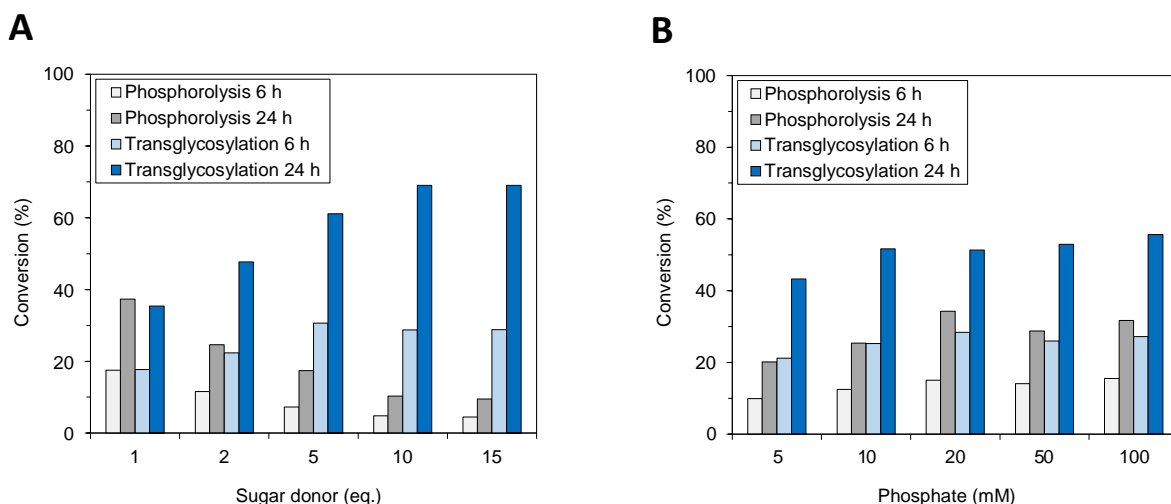


Figure S21. Optimization of A) the sugar donor concentration and B) phosphate concentration for the transglycosylation of 5-fluorouracil. 20 mg of immobilized HeTP (3 mg/g) on Gx-EP403/S were added in 1 mL of reaction mixture containing A) 10 mM 5-fluorouracil and the sugar donor (thymidine) in 10 mM phosphate buffer at pH 7.5. B) 10 mM 5-fluorouracil and 20 mM thymidine in phosphate buffer at pH 7. All the reaction were incubated at 37°C for 1 h.

Table S3. Testing the nucleobase concentration, the amount of biocatalyst, and the temperature to improve the transglycosylation yield. The immobilized HeTP on Gx-EP403 (3 mg/g) was added in 1 mL of reaction mixture containing the sugar donor (thymidine) and the nucleobase (5-fluorouracil) in 10 mM phosphate buffer pH 7.5. The reactions were incubated at 37°C for 24 h with shaking.

Biocatalyst	Nucleobase (mM)	Sugar donor	Temperature (°C)	Phosphorolysis (%)	Transglycosylation (%)
20 mg	10	5 eq. (50 mM)	37	17.4	61.1
	20	5 eq. (100 mM)	37	16.5	59.5
	10	1 eq. (10 mM)	37	37.3	35.4
	30	0.33 eq. (10 mM)	37	39.3	13.4
	10	10 eq.	37	16.4	75.0
	10	10 eq.	45	9.6	52.1
60 mg	10	10 eq.	37	16.4	75.0
	10	10 eq.	37	22.0	79.9

Table S4. Testing different nucleobase concentrations for the flow synthesis of Floxuridine. Residence time: 30 min. Flow-rate: 0.06 mL/min. Reactor volume: 1.8 mL. Temperature: 37°C.

Sugar donor (mM)	Nucleobase (mM)	Transglycosylation (%)	Product (mM)
100	10	87 1	8.7
	20	39 2	7.8
	50	17 1	8.5

Table S5. Scale-up flow synthesis of Floxuridine. Residence time: 45 min. Flow-rate: 0.04 mL/min. Reactor volume: 1.8 mL. Temperature: 37°C.

Nucleobase (mM)	Sugar donor (mM)	Transglycosylation (%)	Product (mM)
10	100	85 2	8.5
20	200	84 2	16.8

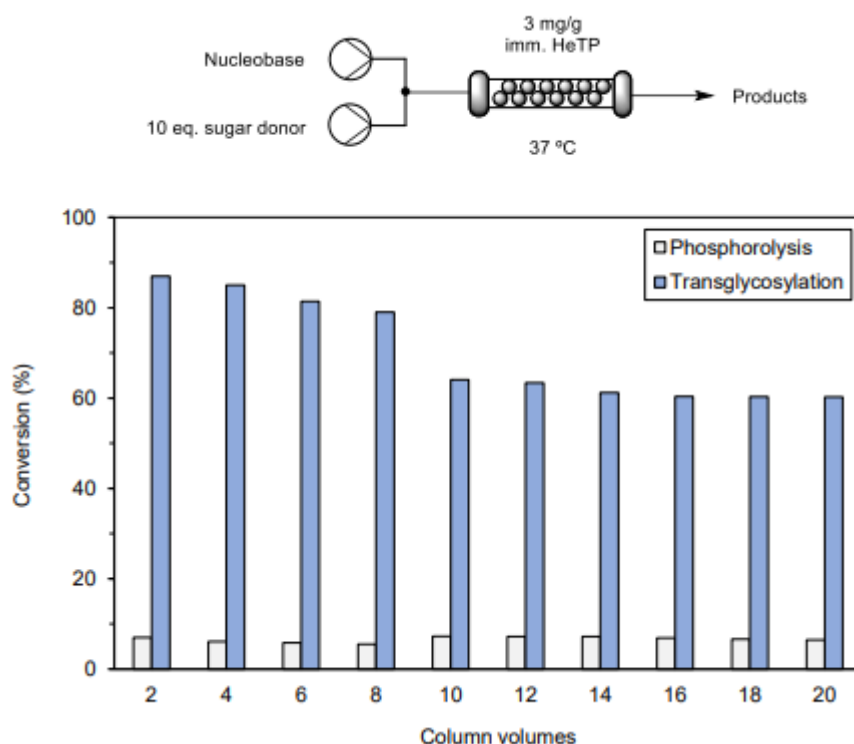


Figure S22. Operational stability of the immobilized HeTP on Gx-EP403/S (3 mg/g) under flow conditions. 10 mM 5-fluorouracil and 100 mM thymidine in 10 mM phosphate buffer at pH 7.5 were pumped to the PBR. Residence time: 30 min. Flow-rate: 0.06 mL/min. Reactor volume: 1.8 mL. Temperature: 37°C.

Supporting references

- 1 E. Mitsiki, A. C. Papageorgiou, S. Iyer, N. Thiyagarajan, S. H. Prior, D. Sleep, C. Finnis and K. R. Acharya, *Biochem. Biophys. Res. Commun.*, 2009, **386**, 666–670.
- 2 V. Timofeev, Y. Abramchik, N. Zhukhlistova, T. Muravieva, I. Fateev, R. Esipov and I. Kuranova, *Acta Crystallogr. Sect. D*, 2014, **70**, 1155–1165.
- 3 D. K. Rogstad, J. L. Herring, J. A. Theruvathu, A. Burdzy, C. C. Perry, J. W. Neidigh and L. C. Sowers, *Chem. Res. Toxicol.*, 2009, **22**, 1194–1204.
- 4 Y. Zhang, J. Sun, Y. Gao, L. Jin, Y. Xu, H. Lian, Y. Sun, Y. Sun, J. Liu, R. Fan, T. Zhang and Z. He, *Mol. Pharm.*, 2013, **10**, 3195–3202.
- 5 M. B. Méndez, J. A. Trelles and C. W. Rivero, *AMB Express*, 2020, **10**, 4–11.
- 6 D. Roura Padrosa, V. Marchini and F. Paradisi, *Bioinformatics*, 2021, **37**, 2761–2762.